ACS BIO & MED CHEM Au
AN OPEN ACCESS JOURNAL OF THE AMERICAN CHEMICAL SOCIETY

pubs.acs.org/biomedchemau
Article

Exploring the Effects of Incorporating Different Bioactive Phospholipids into Messenger Ribonucleic Acid Lipid Nanoparticle (mRNA LNP) Formulations

Published as part of ACS Bio & Med Chem Au special issue "2024 Rising Stars in Biological, Medicinal, and Pharmaceutical Chemistry".

Sunny P. Chen, Shuangyu Wang, Suiyang Liao, and Anna K. Blakney*

Cite This: *ACS Bio Med Chem Au* 2025, 5, 154−165
Read Online

ACCESS | Metrics & More | Article Recommendations | Supporting Information

ABSTRACT: The current rapid advancement in ribonucleic acid (RNA) therapeutics research depends on innovations in drug delivery, especially the development of a lipid-nanoparticle (LNP)-based system. The conventional LNP formulation typically contains four components, including an ionizable cationic lipid, a phospholipid, cholesterol or a cholesterol derivative, and poly(ethylene glycol) (PEG)-lipid, with each contributing to the formulation's overall stability and effectiveness. Among these four types of lipids, the phospholipid component is often known to provide structural support for the nanoparticles but is also a class of bioactive molecules with strong cell signaling potential. This study explores the possibility of incorporating some known structurally related bioactive phospholipids as the fifth component of a conventional four-component LNP formulation and assesses the impacts of such an approach on the physicochemical properties and biological functions of the mRNA LNP formulation. We screened a library of mRNA LNP formulations containing 7 different structurally related bioactive phospholipids at molar concentrations of 5%, 15% and 30% in addition to a conventional four-component LNP formulation (base). We observed differences in physicochemical properties between the mRNA LNP formulations that could be attributed to both the types of phospholipids examined and the molar concentrations used. Cryo-EM analysis revealed structural similarity between the Base formulation and the other formulations. We also characterized the protein expression level in HeLa cells and picked up a distinct cytokine panel signature for each formulation in human peripheral blood mononuclear cells (hPBMCs). Further immunophenotyping analysis showed that most cells that were transfected were CD4+ T cells, and the addition of the different bioactive phospholipids slightly altered cellular tropism. This exploratory study illustrates how adding the bioactive phospholipid can be used to modulate the LNP function, further expanding the design space for RNA LNP formulations and potentiating LNPs for use as RNA therapeutics.

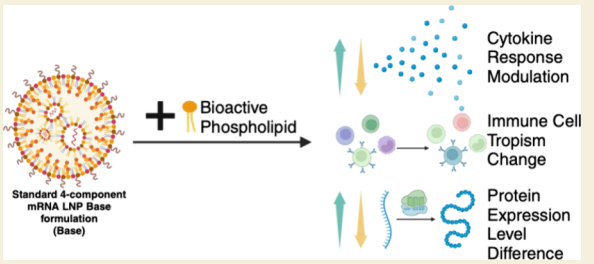

KEYWORDS: *Lipid nanoparticles, Bioactive phospholipids, RNA therapeutics, Phosphatidic acid, Lysophosphatidic acid, Lysophosphatidylcholine, Phosphatidylserine*

1. INTRODUCTION

The current advancement in ribonucleic acid (RNA) therapeutics research, represented by the approval of therapeutics including Onpattro[1] and Coronavirus disease 2019 (COVID-19) RNA vaccines and the mRNA-based respiratory syncytial virus (RSV) vaccine from Moderna,[2−4] relies on breakthroughs in the field of drug delivery, especially the development of lipid-nanoparticle (LNP)-based formulation. RNA is a vulnerable, anionic molecule that requires LNPs to protect them from extracellular degradation and to ensure their delivery to the cells. The conventional clinically approved LNP formulations typically contain four types of lipids, including an ionizable cationic lipid, phospholipid, cholesterol or a cholesterol derivative, and poly(ethylene glycol) (PEG) lipid, with each component contributing to the overall stability and effectiveness of LNPs.[5−7] Briefly, the ionizable lipid is responsible for complexing the anionic RNA and the pH sensitivity facilitates the endosomal escape of the RNA.[5] The phospholipid stabilizes the structure of the LNPs during the particle formation process and may also have a role in endosomal escape.[5,6] The cholesterol, or its derivatives, stabilizes the particles by modulating the membrane integrity

Received: September 1, 2024
Revised: November 18, 2024
Accepted: November 19, 2024
Published: November 27, 2024

and rigidity;[5] and the PEGylated lipid prolongs the circulation time of the LNPs, reduces their size and prevents aggregation.[6]

Besides their structural function in LNPs, each of the four components has an immunomodulatory role that may help improve the overall effectiveness of LNPs,[7] although the exact underlying mechanisms have not been fully elucidated. While the ionizable lipid component and the PEG-lipid component have been studied more extensively for their roles in eliciting the inflammatory response, including the antibody response associated with the LNPs, the immunomodulatory effects of the phospholipid and cholesterol in the context of LNPs have remained largely unexplored.[7] Some studies have demonstrated that varying the phospholipid type or adding another bioactive phospholipid (phosphatidylserine in most cases) component to the standard four-component formulation may enhance transfection efficiency *in vitro*, as well as enhance certain organ-targeting capabilities or even change the biodistribution *in vivo*,[8−13] presenting the possibility of incorporating other bioactive phospholipid candidates to modulate the functionalities of RNA LNP formulations. Since many phospholipids have immunomodulatory functions,[14] we hypothesized that incorporating different bioactive phospholipid candidates at various molar concentrations into a standard four-component LNP formulation could modulate the functionality of mRNA LNP formulations.

Previous literature has also demonstrated that structural differences in lipid molecules can influence their immunomodulatory effects. For example, Miao et al. showed that the empty LNPs (eLNPs, LNPs without any RNA cargo) formulated with a heterocyclic ionizable cationic lipid upregulated certain immune activation markers such as CD40 and MHCII in mouse bone-marrow-derived dendritic cells as compared to eLNPs formulated with a linear ionizable cationic lipid.[15] Nguyen et al. showed that only lyso-PS nanoparticles were able to induce oral tolerance in mice as compared to double-chain-PS nanoparticles.[16] Similarly, Pizzuto et al. showed that the degree of saturation of acyl chain of cardiolipin impacts its ability to elicit proinflammatory cytokines including TNF-α and IL-1β.[17]

Herein, we screened a library of mRNA LNP formulations containing 7 different bioactive phospholipids at molar concentrations of 5%, 15% and 30%. These phospholipids were chosen based on their immunomodulatory potential previously documented in the literature,[17−20] with variations in the structure (e.g., the headgroup) to better understand the effect of phospholipid structure on LNP function. We aimed to determine how incorporating these bioactive phospholipids into the Base formulation, which is a standard 4-component LNP formulation derived from an optimized formulation developed by our group before[21] at various molar concentrations, impacts the physicochemical properties of the mRNA LNP formulations and their biological functions. We observed differences in physicochemical properties between the mRNA LNP formulations that could be attributed to both the types of phospholipids examined and the molar concentrations used. Furthermore, we characterized the level of protein expression in HeLa cells and the distinct cytokine panel signature, as well as the types of the immune cells transfected, for each formulation in human peripheral blood mononuclear cells (hPBMCs).

2. MATERIALS AND METHODS

2.1. mRNA Synthesis

2.1.1. pDNA Linearization. The mRNA plasmid DNA (pDNA) encoded enhanced green fluorescent protein (eGFP) with tobacco mosaic virus (TMV) 5′ and 3′ UTRs. The pDNA was transformed into *Escherichia coli*, cultured overnight in 100 mL of LB broth with 50 μg/mL carbenicillin (Thermo Fisher Scientific). The pDNA was isolated and purified using the QIAGEN Plasmid Plus Maxi Kit (QIAGEN), according to the manufacturer's protocols. The pDNA concentration was measured using NanoDrop. 2.5 μg of the pDNA was linearized with 2 μL of AscI per 20 μL reaction, incubated at 37 °C for 2 h, and the reaction was heat inactivated by incubating at 80 °C for 20 min.

2.1.2. In Vitro Transcription, Capping, and Purification of eGFP mRNA. A reaction including 1 μg of the linearized eGFP mRNA pDNA was used to synthesize mRNA via *in vitro* transcription per 20 μL reaction with 40 mM Tris-HCL (pH 8.0, Thermo Scientific) and 10 mM dithiothreitol (DTT, Thermo Scientific), 42 mM magnesium acetate (Sigma-Aldrich), 2 mM spermidine (Thermo Scientific), 7.78 mM ATP, GTP and CTP (Thermo Scientific NTP Set, Thermo Scientific), 7.78 mM N1-methyl-pseudo UTP (Hongene Biotech), 4 U T7 RNA polymerase (NEB), 1 U murine RNase inhibitor (NEB), 0.002 U inorganic pyrophosphatase from yeast (Hongene Biotech), and ultrapure DNase/RNase free distilled water (Thermo Fisher Scientific). The reaction was incubated at 37 °C for 2 h. The resulting mRNA was purified by the lithium chloride purification method, which involved adding an equal volume of lithium chloride (LiCl) precipitation solution (AM9480, Thermo Fisher Scientific) and incubating overnight at −20 °C. The yielded mRNA was pelleted by centrifugation at 13,000*g* at 4 °C, and the pellets were washed with 70% ethanol, dried at room temperature, and hydrated with nuclease-free water. The uncapped mRNA concentration was measured using NanoDrop.

Post-transcriptional capping reactions were carried out using the ScriptCap Cap 1 Capping System (CELLSCRIPT) per the manufacturer's instructions. After incubation, the capped mRNA was purified again by the lithium chloride purification method, as described above. The purified capped mRNA was resuspended in nuclease-free water, with the concentration being measured by NanoDrop and stored at −70 °C until use.

2.2. mRNA LNP Formulation and Storage

2.2.1. Lipid Component Stock Solution Preparation. ALC-0315 (BroadPharm, Catalog. BP-25498) was solubilized in 100% ethanol at 40 mg/mL, 18:1 (Δ9-Cis) PE (DOPE) (Avanti Polar Lipids, 850725P), plant cholesterol (Caymen Chemical Company, 39448), DMG-PEG 2000 (Avanti Polar Lipids, 880151P), and lysophosphatidylcholine (lyso PC) 18:1 (Avanti Polar Lipids, 845875P) were solubilized in 100% ethanol at 20 mg/mL. Cardiolipin (CL) 18:1 (Avanti Polar Lipids, 710335P) was solubilized in 100% ethanol at 13.3 mg/mL. Lysophosphatidic acid (lyso PA) 18:1 (Avanti Polar Lipids, 857130P) was solubilized in 50% ethanol (ethanol: water 1:1 v/v) at 20 mg/mL. Phosphatidic acid (PA) 18:1 (Avanti Polar Lipids, 840875P) was solubilized in a mixture of tetrahydrofuran (THF, Thermo Fisher Scientific, 348451000) and ethanol (THF: EtOH 3:2, v/v) at 20 mg/mL. Phosphatidylserine (PS) 18:1 (DOPS, Avanti Polar Lipids, 840035P) was solubilized in a mixture of THF and ethanol (THF: EtOH 4:1, v/v) at 20 mg/mL. Cardiolipin 18:0 (Avanti Polar Lipids, 710334P) was solubilized in 100% ethanol at 1 mg/mL and PA 18:0 (Avanti Polar Lipids, 830865P) was solubilized in 100% methanol at 1 mg/mL. The stock solutions were stored at −20 °C until use.

2.2.2. mRNA LNP Formulation. We employed a full factorial design of experiment (DoE) approach to construct our library of LNP formulations, varying the phospholipid types and their molar concentrations in the formulation. The molar percentage of each component of LNP formulation varies according to Table 1.

The organic phase was prepared at a concentration of 19.5 mM for the Base formulation and all the formulations containing lyso PC

https://doi.org/10.1021/acsbiomedchemau.4c00085
ACS Bio Med Chem Au 2025, 5, 154−165

Table 1. Molar Percentage of mRNA LNP Formulations

	Base	5% Bioactive Phospholipid	15% Bioactive Phospholipid	30% Bioactive Phospholipid
ALC-0315	45%	42.75%	38.25%	31.5%
DOPE	17.5%	16.62%	14.88%	12.25%
Cholesterol	36.25%	34.44%	30.81%	25.37%
DMG-PEG 2000	1.25%	1.19%	1.06%	0.87%
Bioactive Phospholipid	N/A	5%	15%	30.01%

18:1, cardiolipin 18:1, lyso PA 18:1, PA 18:1, and PS 18:1. For the formulations containing cardiolipin 18:0 and PA 18:0, the organic phase was prepared at a concentration of 5 mM, and a Base formulation was also prepared at a concentration of 5 mM as a reference. Note that for the formulations containing cardiolipin 18:0, only 5% cardiolipin 18:0 formulation was possible; for the formulations containing PA 18:0, only 5% and 15% PA 18:0 formulations were possible. This is due to their low soluble concentration in the stock solution (1 mg/mL). The organic phase for each concentration was prepared by mixing the lipid component stock solutions while maintaining a homogeneous solution. The aqueous phase was prepared by diluting the stock eGFP mRNA in 25 mM sodium acetate at pH 4.

The mRNA LNPs were formulated by microfluidic mixing via a T-tube.[8,21] The organic and the aqueous phases were combined at a N:P ratio of 10:1 between the ionizable lipid and RNA, and a flow rate of 1:3, respectively, using a total flow rate of 16 mL/min. Immediately after the mixing, the mRNA LNPs were diluted 10-fold using 1× PBS (pH 7.4, Thermo Fisher Scientific), and were concentrated and purified using sterilized MWCO 10 kDa centrifugal filters (Amicon, Millipore Sigma) at 4 °C and 2200*g* until the total volume was reduced ∼20−40-fold to between 0.2 and 1.5 mL. For each formulation, an aliquot of fresh LNPs was used for dynamic light scattering (DLS), electrophoretic light scattering (ELS) and RiboGreen analysis; the remaining were aliquoted and stored in 10% sucrose PBS solution at −20 °C until ready to use.

2.3. Characterization of mRNA LNP Physicochemical Properties

2.3.1. DLS and ELS Analysis. LNP size, polydispersity index (PDI) and zeta potential were measured using the Zetasizer Nano (Malvern Instruments) and Zetasizer 7.12 software (Malvern) as described previously.[21] mRNA LNPs were diluted up to 200-fold in PBS before the analysis.

2.3.2. LNP Encapsulation Efficiency. The RiboGreen assay was conducted using a Quant-iT Ribogreen RNA Assay Kit (Invitrogen, Thermo Fisher Scientific) to determine the encapsulation efficiencies of LNP formulations. The assay was carried out as per instruction and as described previously.[21] The encapsulation efficiency (EE) was calculated based on the following:

$$\text{EE\%} = \frac{\text{mass of encapsulated mRNA}}{\text{total mass of mRNA detected in the sample}} \times 100\%$$

The mRNA LNP concentrations were based on the calculated encapsulated mRNA.

2.3.3. Cryo-EM. The thawed LNPs were concentrated to approximately 20 mg/mL total lipid concentration and applied (3−5 μL) to glow-discharged copper grids. These grids were plunge-frozen in vitreous ice using an FEI Mark IV Vitrobot (FEI, Hillsboro, USA). Subsequently, grids were transferred to a Gatan 70° cryotilt holder, pre-equilibrated to at least −180 °C, and loaded into the microscope. Imaging was conducted on an FEI LaB6 G2 TEM (FEI, Hillsboro, OR), operating at 200 kV under low-dose conditions with an FEI Eagle 4 K CCD camera. All samples were captured at a magnification of 55,000× with a nominal under-focus of 1−2 μm to improve contrast. Sample preparation and imaging were carried out by the UBC Bioimaging Facility (Vancouver, BC).

2.4. HeLa Cell Culture, Passage, and Transfection

HeLa cells were maintained in completed Dulbecco's Modified Eagle Medium (C-DMEM) containing DMEM (Gibco, Thermo Fisher Scientific, 11960069), with 1% glutaMAX (Gibco, Thermo Fisher Scientific, 35050061), 1% penicillin-streptomycin (Gibco, Thermo Fisher Scientific, 15070063) and 10% fetal bovine serum (FBS, Gibco, Thermo Fisher Scientific, 12483020).

For the transfection efficiency test, HeLa cells were seeded at 6-well TC-treated plates at 300,000 cells/well density in 2 mL of C-DMEM. After ∼24 h of seeding, the old media was removed and replaced with 1.6 mL of Opti-MEM media (Gibco, Thermo Fisher Scientific, 11058021). The mRNA LNP formulations were thawed, with 5 μg of mRNA diluting in 400 μL of Opti-MEM media. The Opti-MEM-LNP mixtures were then added to the wells. Flow cytometry was performed ∼24 h post-transfection to assess the transfection efficiency, using a viability dye (LIVE/DEAD Fixable Far Red Dead Cell Stain Kit, for 633 or 635 nm excitation, Invitrogen, Thermo Fisher Scientific, L34974).

2.5. Human Peripheral Blood Mononuclear Cell Isolation and LNP Transfection

All hPBMC studies were conducted following the University of British Columbia human ethical protocol H22−00584. Bags of four-donor-pooled residual buffy coats were ordered from the Canadian Blood Services (Vancouver, BC). For the cytokine response analysis, the product was composed of three males and one female, ages 24 to 70. For the immunophenotyping analysis, the product was composed of two males and two females, ages 19 to 60. The fresh hPBMCs were isolated by density gradient centrifugation using Lymphoprep (STEMCELL Technologies, 07581). After two washes with DPBS containing 2% FBS, the red blood cells were lysed using ammonium chloride solution (STEMCELL Technologies, 07850) and the platelets were reduced by low-speed centrifugation without a brake (120*g*). The freshly isolated hPBMCs were cultured in 6-well TC-treated plates at ∼7 M cells/well density in 3 mL completed RPMI-1640 media containing RPMI 1640 (no glutamine, Gibco, Thermo Fisher Scientific, 21870092), with 1% glutaMAX (Gibco, Thermo Fisher Scientific, 35050061), 1% penicillin-streptomycin (Gibco, Thermo Fisher Scientific, 15070063) and 10% fetal bovine serum (FBS, Gibco, Thermo Fisher Scientific, 12483020).

After the overnight culture, the old media was replaced with 1.6 mL of Opti-MEM media (Gibco, Thermo Fisher Scientific, 11058021). The mRNA LNP formulations were thawed, with 0.5 μg of mRNA diluting in 400 μL of Opti-MEM media per well of transfection. The Opti-MEM-LNP mixtures were then added to the wells.

For the immunophenotyping purpose, 100 μL of the LNP-mRNA of each formulation in a final concentration of ∼0.156 μM were stained using SYTO 13 Green Fluorescent Nucleic Acid Stain (Invitrogen, Thermo Scientific, S7575) in a final concentration of 1.7 μM. After direct mixing with the dye and incubating at 4 °C for 40 min, the mRNA LNP formulations were diluted 10-fold using 1× PBS (pH 7.4, Thermo Fisher Scientific), and were washed using sterilized MWCO 10 kDa centrifugal filters (Amicon, Millipore Sigma) at 4 °C and 2200*g* until the total volume was similar to the original starting volume (e.g., 100 μL). A 0.5 μg equivalent of each stained mRNA LNP formulation was used to validate the binding of the dye to the encapsulated RNA by measuring the fluorescence intensities at an excitation wavelength of 485 nm and emission wavelength of 535 nm. After the validation, similar steps were followed for transfecting the hPBMCs (0.5 μg of mRNA diluting in 400 μL of Opti-MEM media per well of transfection).

2.6. Cytokine Analysis

After ∼20 h post-transfection, the hPBMC supernatant was collected and stored at −70 °C for the downstream cytokine analysis. The Meso Scale Discovery (MSD) U-PLEX custom human biomarker assays (K15067M-1) and the U-PLEX human TGF-β combo assays (K15241K-1) were used to assess the various cytokine levels in response to the mRNA LNP transfection per manufacturer's instructions. The cytokines under investigation include IFN-γ, IL-

https://doi.org/10.1021/acsbiomedchemau.4c00085
ACS Bio Med Chem Au 2025, 5, 154−165

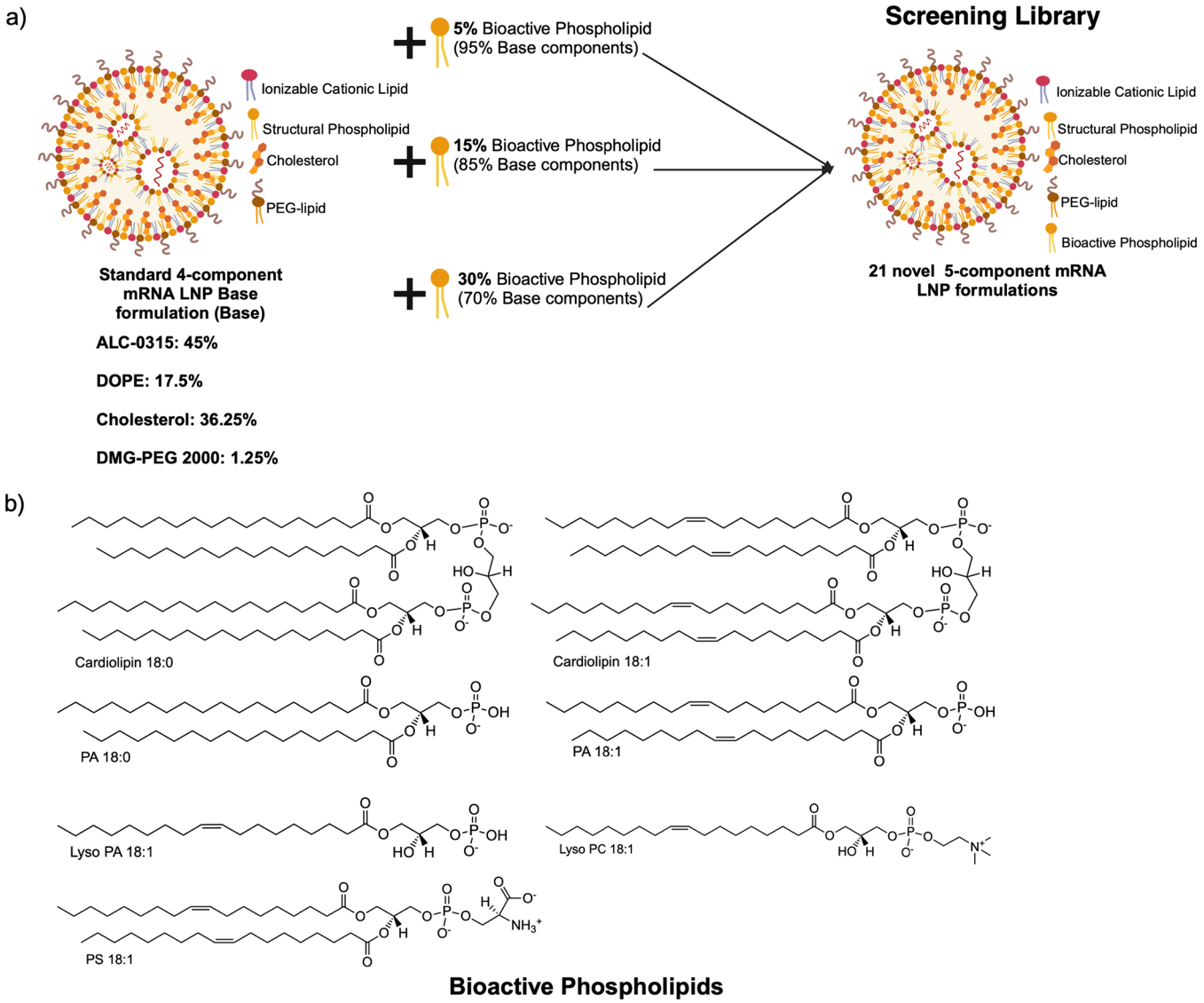

Figure 1. Schematic of bioactive phospholipid LNP library construction. (a) The LNP formulation library was constructed by adding 1 of the 7 bioactive phospholipids into the Base formulation at molar concentrations of 5%, 15%, and 30%. (b) Chemical structures of the bioactive phospholipid used in this study.

1α, IL-1β, IL-2, IL-4, IL-5, IL-6, IL-10, IL-12p40, IL-13, IL-17A, IP-10, TNF-α, TGF-β1, and TGF-β2.

2.7. Immunophenotyping

After ∼15−20 h post-transfection, the hPBMCs were harvested, with the adherent portion being harvested using 5 mM ice-cold EDTA, incubating on ice for at least 30 min, and extensive pipetting. Both the suspension and the adherent portion of the hPBMCs were resuspended in a total of 1 mL of FACS buffer (1× PBS and 2% FBS). Cell densities were determined, and ∼1 M cells from each sample were aliquoted for downstream antibody staining. These cells were resuspended in 100 μL of FACS buffer and were treated with Human TruStain FcX (BioLegend, 422302) to avoid unspecific bindings before applying the antibody cocktail staining, following the manufacturer's recommendations. The cells were stained using the antibody cocktail (Table S1) in the dark for 30 min at 4 °C, washed twice using 1X FACS buffer and analyzed using a CytoFLEX LX cytometer (Beckman Coulter) and Flowjo software (version 10.10.0).

2.8. Statistical Analysis

All of the DoE-relevant statistical analysis was performed using JMP (version 18.0.1). In brief, a full factorial DoE design option was selected with 2 input factors (bioactive lipids including all the 18:1 phospholipids and molar percentage at 0%, 5%, 15% and 30%) and 4 output factors (size, PDI, zeta-potential, and EE). A predictor screening was then utilized to evaluate how the different types of bioactive phospholipid incorporated and the various levels of incorporated molar percentages (the "predictor") impact the physicochemical property parameters assessed (the "response"). Other statistical analysis was performed using GraphPad Prism 10.2.3. The statistical tests used were specified in the figure legends.

3. RESULTS AND DISCUSSION

3.1. Physicochemical Property Assessment of Bioactive Phospholipid mRNA LNP Formulations via a Design-of-Experiment (DoE) Approach

As illustrated in Figure 1a, our library of mRNA LNP formulations was constructed by incorporating 7 different bioactive phospholipids into the Base LNP formulation (Base), respectively, at molar concentrations of 5%, 15%, and 30%. This is a full-factorial design of experiment approach to construct the library, which would provide a rationale for future design if any trend could be observed between the

https://doi.org/10.1021/acsbiomedchemau.4c00085
ACS Bio Med Chem Au 2025, 5, 154−165

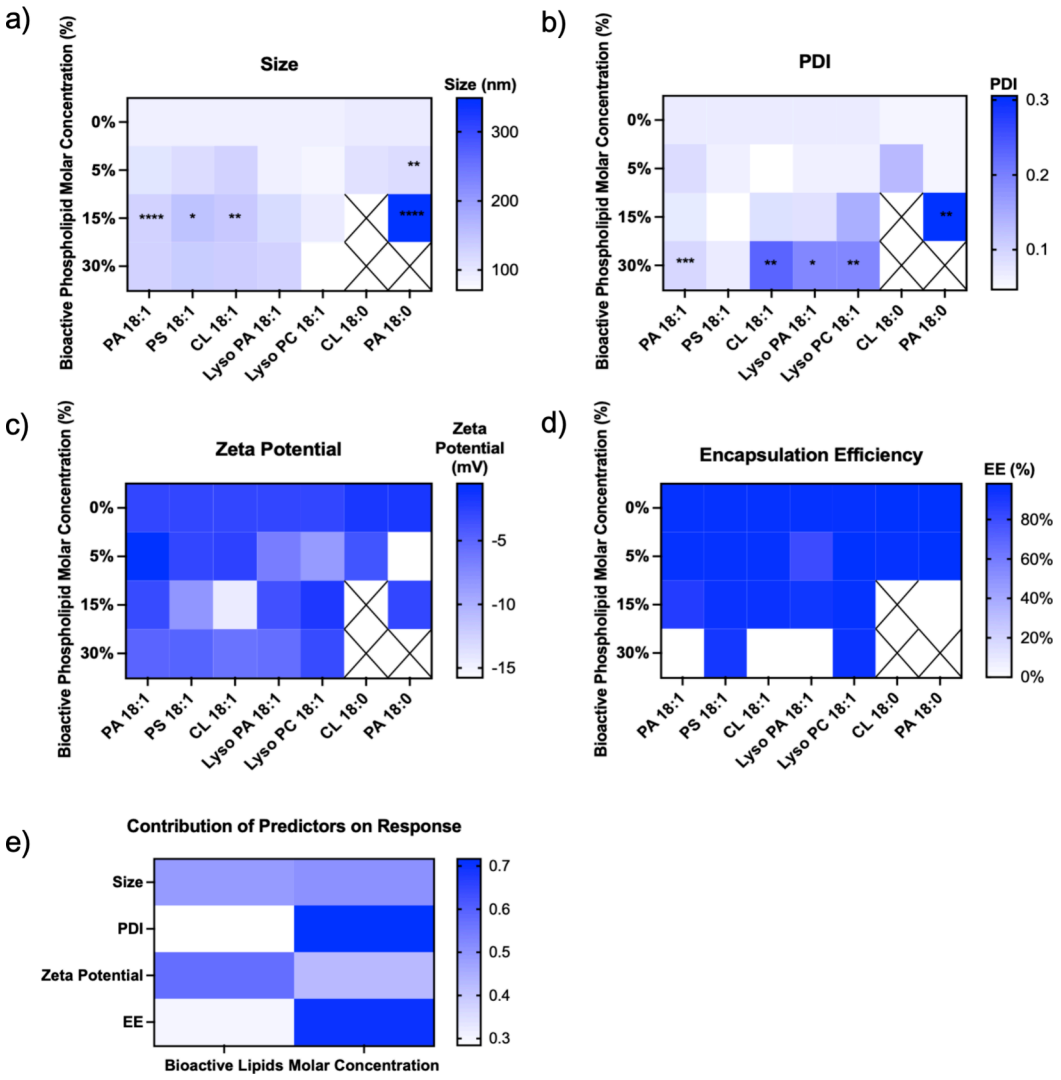

Figure 2. Physicochemical property assessment of all of the formulations in the library. The Base formulation was prepared as the control (0% bioactive phospholipid). (a) Heatmap illustrating the particle size of the formulations measured by DLS analysis. (b) Heatmap illustrating the polydisperse index of the formulations measured by DLS analysis. (c) Heatmap illustrating the zeta potential measured by ELS analysis. (d) Heatmap illustrating the EE measured by RiboGreen assay. Note that only formulations that demonstrated EE > 80% were included for the biological function test next. (e) Heatmap showing the predictor screening analysis result from JMP that determines how incorporating different kinds of bioactive lipids at different molar concentrations impacts the physicochemical properties of the particles including size, PDI, zeta potential and EE. Statistical analysis was conducted using the 2-way ANOVA test followed by Tukey's multiple comparison test. Heatmap squares represent means for $n = 3$ replicates. Level of significance compared to the Base formulation (0%): $^{*}p \leq 0.05$, $^{**}p \leq 0.01$, $^{***}p \leq 0.001$, $^{****}p \leq 0.0001$.

incorporated phospholipid type, the molar concentration, and the resulting physicochemical properties. The quality of mRNA was validated before formulation (Figure S1). The Base represented a conventional four-component LNP formulation, which had molar percentages of ALC-0315: DOPE: Cholesterol: PEG-2000 at 45:17.5:36.25:1.25, and is a formulation derived from an optimized formulation developed by Ly et al. previously from our group,[21] that has achieved optimal Critical Quality Attributes (CQAs). The 7 bioactive phospholipids under investigation were CL 18:0, CL 18:1, PA 18:0, PA 18:1, lysoPA 18:1, PS 18:1, and lysoPC 18:1 (Figure 1b). We studied the effects of incorporating different molar percentages of these bioactive phospholipids on the physicochemical properties of the resulting mRNA LNP formulations, including size, polydisperse index (PDI), zeta-potential, and encapsulation efficiency. Due to solubility limitations, we could not formulate CL 18:0 into the 15% and 30% formulations and PA 18:0 into the 30% formulation. Therefore, we prepared 18 LNP formulations, as listed in Table S2.

By performing dynamic light scattering (DLS) analysis, we observed that the particle sizes for all the formulations, except the 15% PA 18:0 formulation, ranged from 70−120 nm. The 15% PA 18:0 formulation resulted in large particles with an average diameter of ∼350 nm. Particles increased in size as the molar concentration of the incorporated bioactive phospholipid increased (Figure 2a), irrespective of the incorporated bioactive phospholipid type. All of the formulations, except the 15% PA 18:0 formulation, had a PDI of less than 0.2, indicating that the particle size for each formulation was relatively uniform. As a general trend, the PDI also increased as the molar concentration of the incorporated bioactive phospholipid increased (Figure 2b), which was irrespective of the incorporated phospholipid type. These observed

https://doi.org/10.1021/acsbiomedchemau.4c00085
ACS Bio Med Chem Au 2025, 5, 154−165

phenomena might be partly attributed to the reduced molar concentration of the DMG-PEG component used in the formulation, in response to the increased molar percentages of the incorporated bioactive phospholipids, as literature has reported decreased particle size with increased PEG content[22] and PEG content is known to impact the dispersity of particle population.[23] The large PDI (∼0.3) from the 15% PA 18:0 formulation is probably related to the poor solubility of PA 18:0 in ethanol. The phospholipid did not remain in solution after mixing of the organic phase and the aqueous phase, resulting in the formation of aggregates.

By performing electrophoretic light scattering (ELS) analysis, the zeta potential was determined for each formulation. The zeta potential for the formulations ranged from near neutral (∼-2 mV) to slightly negative (∼-10 mV) with no clear trend observed (Figure 2c).

The encapsulation efficiency (EE) for each formulation was determined by a RiboGreen assay. All the formulations had an EE of at least 80% except the 30% PA 18:1 formulation, the 30% CL 18:1 formulation, the 30% lyso PA 18:1 formulation and the 15% PA 18:0 formulation, which had no mRNA encapsulated at all (Figure 2d). Thus, at the 30% molar concentration level, only the PS 18:1 and lyso PC 18:1 formulations had encapsulated mRNA. This observation might be partly attributed to charges carried by the different bioactive phospholipids. PA 18:1, lyso PA 18:1, PA 18:0 and CL 18:1 all have only negatively charged head groups while PS 18:1 and lyso PC 18:1 have positively charged moieties in addition to the negatively charged moieties in their head groups (Figure 1b). It is possible that negatively charged phospholipids compete with the mRNA molecules for binding to the ionizable cationic lipid. At the 30% molar concentration level for the bioactive phospholipid, the molar concentration for the ionizable cationic lipid is at 31.5% (Table 1), this almost 1:1 ratio might have saturated all the ionizable cationic lipid for binding the negatively charged bioactive phospholipids and impaired mRNA binding. On the other hand, because of the positively charged moieties, the head groups from PS 18:1 and lyso PC 18:1 could provide additional complexation with mRNA, enabling adequate encapsulation.

We also performed a predictor screening analysis using JMP 18 to determine how the different types of bioactive phospholipid incorporated and the various levels of incorporated molar percentages (the "predictor") impact the physicochemical property parameters assessed (the "response") (Figure 2e). The particle size was equally affected by the type of phospholipid incorporated and the molar percentage incorporated. On the other hand, the PDI and EE were more impacted by the molar percentage incorporated. The zeta potential was more affected by the type of phospholipid incorporated.

Since 4 formulations did not meet the CQA for mRNA encapsulation (>80%), they were excluded from further analysis. The remaining 14 formulations (Table 2) proceeded to be tested further. Cryo-EM analysis of the formulations revealed that these formulations largely resembled structural similarity to the Base formulation, with observable "bleb" structures (Figure S2),[24] which are understood as aqueous compartments where the nucleic acid cargo could potentially reside and might be a desired feature associated with improved transfection potency.[25] Note that 5% and 15% lyso PC 18:1 formulations have larger "blebs" as compared to the Base formulation (Figure S2a, n, and o).

Table 2. 14 Formulations with Sufficient CQAs Used for Biological Assays

Bioactive Phospholipid	Molar Percentage
PA 18:1	5%
	15%
PS 18:1	5%
	15%
	30%
CL 18:1	5%
	15%
Lyso PA 18:1	5%
	15%
Lyso PC 18:1	5%
	15%
	30%
CL 18:0	5%
PA 18:0	5%

3.2. Transfection Efficiency and eGFP Protein Expression Test in HeLa Cells

We tested the capacity of the mRNA LNP formulations to deliver RNA by transfecting HeLa cells and performed a flow cytometry analysis of the cellular eGFP expression level. All 14 formulations transfected the HeLa cells at a similar level (∼90%) compared to the Base formulation (Figure 3a). The 5% PA 18:0 formulation had the lowest level of viable eGFP-positive cells (∼88.3%) among all the formulations but the highest level of both the total dead cell frequency and the eGFP-positive dead cell frequency (Figure S3a, b), suggesting that there is mild cytotoxicity associated with this formulation. This is expected as literature has demonstrated that PA 18:0 could mediate lipotoxicity through accumulating in the cell ER and inducing ER stress.[26] In contrast, 5% and 15% lyso PA 18:1 formulations both had lower total dead cell frequencies than the media-only control ("UT", untransfected), which might be explained by the intrinsic capacity of lyso PA to induce cell proliferation, especially in epithelial cancer cell lines as documented.[27,28]

Despite similar levels of HeLa cell transfection between the formulations, we observed some differences in the protein expression (Figure 3b). We observed a ∼ 2-fold increase in MFI in the 15% and 30% PS 18:1 formulations, consistent with the existing literature that reports that PS nanoparticles can induce higher protein expression in other human epithelial cell lines including 1HAEo[8] and Huh-7.[29] However, no MFI fold increase could be observed for the 5% PS 18:1 formulation, suggesting that the effect is dependent on the bioactive phospholipid molar percentage. Besides the 15% and 30% PS 18:1 formulations, the 15% lyso PA 18:1, and 5% and 15% lyso PC 18:1 formulations resulted in an ∼1.6-fold increase in MFI, while the 5% PA 18:0 and 15% PA 18:1 formulations could result in ∼1.4-fold increase in MFI (Figure 3b). On the other hand, both 5% lyso PA 18:1 and 30% lyso PC 18:1 formulations resulted in MFI that was ∼40% lower than the Base formulation, emphasizing again that cellular protein expression of the transfected mRNA LNP formulations depends on both the incorporated bioactive phospholipid type and the molar percentage incorporated. The enhanced protein expression observed with the 5% and 15% lyso PC 18:1 formulations might be associated with their seemly larger size of the "bleb" structures as compared to the Base formulation (Figure S2a, n, and o).

https://doi.org/10.1021/acsbiomedchemau.4c00085
ACS Bio Med Chem Au 2025, 5, 154−165

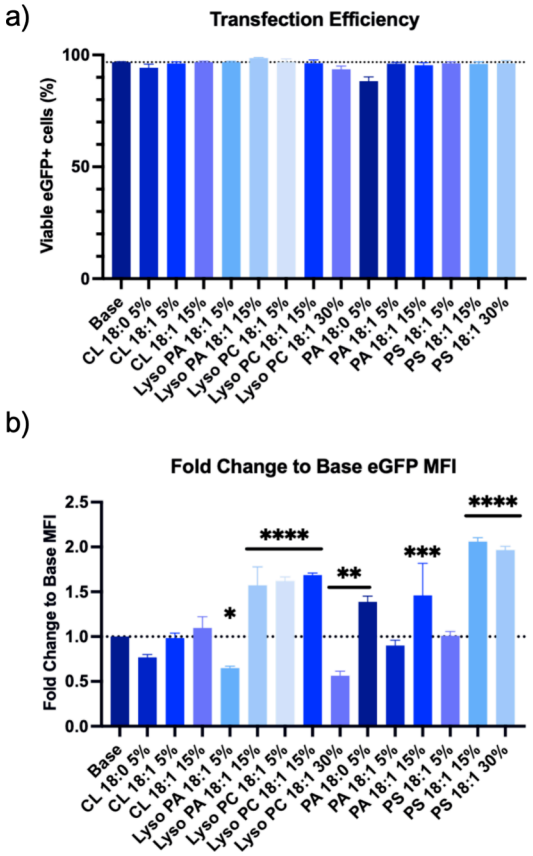

Figure 3. Hela cell transfection of all 14 formulations (5 μg of mRNA LNP eGFP) that showed >80% EE. The Base formulation was included as a control. (a) Transfection efficiency as determined by the viable eGFP+ cell frequency from flow cytometry. Statistical analysis was conducted using the Kruskal–Wallis test followed by Dunn's multiple comparisons test. Bars represent means ± SD, n = 3. (b) Mean fluorescence intensity of cellular eGFP expression normalized against the eGFP expression level from the Base formulation transfection. Up to an ∼2-fold increase could be observed. Statistical analysis was conducted using the ordinary one-way ANOVA test followed by Dunnett's multiple comparison test. Bars represent means ± SD for n = 3. Level of significance compared to the Base formulation: *$p \leq 0.05$, **$p \leq 0.01$, ***$p \leq 0.001$, ****$p \leq 0.0001$.

3.3. Immunomodulatory Effect Assessment via Cytokine Response Analysis and Immunophenotyping Analysis in Human PBMCs

We assessed the immunomodulatory effects associated with the 14 formulations by performing cytokine analysis using Meso Scale Discovery (MSD) U-plex kits on the supernatants from transfected human PBMCs. We analyzed 15 cytokines including IFN-γ, IL-10, IL-12/IL-23p40, IL-13, IL-17A, IL-1α, IL-1β, IL-2, IL-4, IL-5, IL-6, IP-10, TNF-α, TGF-β1 and TGF-β2. These cytokines were chosen based on their implications in LNP-related studies, as well as in the relevant bioactive phospholipid-related studies.[17−20,30−35]

In general, we observed that transfecting the human PBMCs with any mRNA LNP formulations, regardless of the standard 4-component or the 5-component ones, increased the release of TGF-β1 (Figures 4a, S4o). TGF-β signaling has been speculated to activate fatty acid synthesis and might also influence lipid droplet content in certain myeloid cells.[36] Since we are providing the cells with more lipids by transfecting them with LNPs, it is within the expectation that the downstream pathways that are relevant to lipid metabolism will be upregulated. In terms of its immunomodulatory effects, TGF-β signaling is multifaceted, especially in combination with other cytokines including IL-2 and IL-6, which have been shown to influence T cell population differentiation and composition (e.g., Treg vs Th17) and thus the general immune outcomes (e.g., immunosuppressive vs autoimmune).[37]

We also observed that transfecting the cells with formulations with incorporated bioactive phospholipids further increased the release of TGF-β1, which varied between the different formulations (Figures 4a, S4o). In addition to TGF-β1, transfecting the cells with the bioactive phospholipid-incorporated formulations increased the release of IL-12/IL-23p40 (a surrogate IL-12), as well as IL-6, TNF-α, TGF-β2, IFN-γ, IL-10 and IL-1β (Figures 4a, S4b–d, h, l, n, and p). This is a mixed list of "pro"- and "anti-inflammatory" cytokines,[37,38] therefore, the immune outcome is formulation-dependent. For example, the release of IL-6 is often tied to the sensing of the ionizable lipid[39] while IL-10 exerts its anti-inflammatory effects through a lipid-metabolism-related mechanism,[40] which would make the immune outcome unpredictable. Another example would be, PS formulation has been shown to have anti-inflammatory effects by inducing both IL-10 and TGF-β release and inhibiting IL-6 and IL-17 release;[35] however, with the current study, there is an elevated level of IL-6 associated with 30% PS formulation, the highest PS formulation among the three (Figure S4l). The mixed list of cytokines further illustrates the need to tailor formulations for different applications.

By examining each formulation more closely, we observed a dosage-dependent response for the release of IL-10, IL-17A, IP-10, TNF-α (for lyso PC 18:1 formulations only), and TGF-β1(except for PS 18:1 formulations) (Figures 4a, S4c, f, m–o), suggesting a more direct relationship between the bioactive phospholipids incorporated and the cytokines released. For example, the literature suggests that unsaturated CLs are inhibitors of TLR4, which will lead to the reduced release of proinflammatory cytokines such as TNF-α and IP-10.[41] This is consistent with what we observed with 5% and 15% CL 18:1 formulations; there was a decrease in both IP-10 and TNF-α production as the molar percentage of CL 18:1 increased (Figure S4m, n). In addition, we observed an increase in both IL-10 and TGF-β1 production and a decrease in IL-17A production (Figure S4c, f, o) as the molar percentage increased, further suggesting the immunosuppressive potential of this bioactive phospholipid. However, we did not observe the opposite effect from the saturated CL (CL 18:0)[17] in our study, indicating that there are other factors at play. For example, cholesterol metabolism has been shown to impact the expression of TLR4 and lead to increased TNF-α and IL-6,[42] which might interfere with the results to clearly distinguish the functions between CL 18:1 and CL 18:0. For lyso PA 18:1, the literature demonstrated a reduced release of TNF-α,[19] which was not observed in the current study (Figure S4n). However, we observed a positive correlation between both IL-10 and TGF-β1 and the molar percentage of lyso PA 18:1 (Figure S4c, o), which also showed the immunosuppressive potential of the phospholipid. Lyso PC has more diverse functions such as influencing both the conventional T cell function and the regulatory T cell function;[18] therefore, it would be desirable to induce immunomodulation. In our current study, we observed a decrease in the production of IL-10, IP-10, TNF-α, IL-17A and TGF-β1 as the molar percentage of lyso PC 18:1 increased

https://doi.org/10.1021/acsbiomedchemau.4c00085
ACS Bio Med Chem Au 2025, 5, 154–165

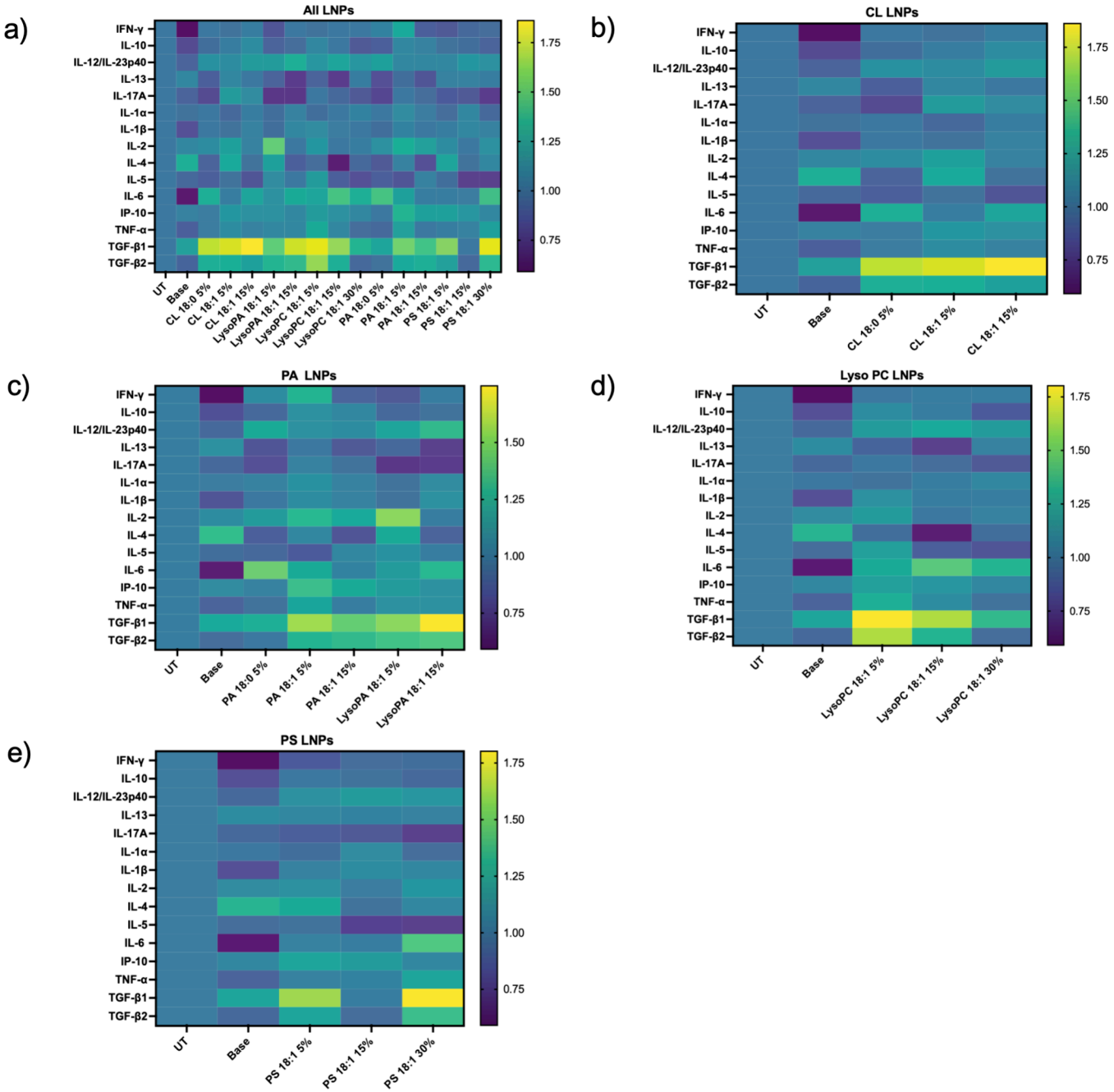

Figure 4. Heatmap of cytokine response from human PBMC transfection of all 14 formulations (0.5 μg of mRNA LNP eGFP) using Meso Scale Discovery human U-plex kits. Fifteen cytokines were measured. The Base formulation was included as a control. All of the values are normalized against the untransfected condition (UT). (a) Heatmap of cytokine response from all the formulations. (b−e) Heatmap of cytokine response split by formulations that share a similar headgroup such that other structural variations and different molar concentrations could be better compared. (b) Heatmap of cytokine response from all the CL formulations as compared to the Base. (c) Heatmap of cytokine response from all the PA formulations as compared to the Base. (d) Heatmap of cytokine response from all the lyso PC formulations as compared to the Base. (e) Heatmap of cytokine response from all the PS formulations as compared to the Base. Statistical analysis was conducted when possible using the 2-way ANOVA test followed by Tukey's multiple comparison test. Heatmap squares represent means for n = 3 for all of the cytokines except IL-6 and IFN-γ when only singlet samples after dilution were within the detection range.

(Figure S4c, f, m−o), which suggested that a specific immunomodulatory aim could be achieved by altering the molar concentration of lyso PC 18:1.

We also inspected the formulation performance by headgroup differences (Figure 4b−e). No clear trend could be observed, except that CL-related lipid formulations (both CL 18:0 and CL 18:1) are stronger inducers of TGF-β1 as compared to other formulations. Lyso PA formulations inhibit the release of IL-13 and IL-17A, with the literature clearly describing the involvement of lyso PA in IL-13 signaling.[43−45] Taken together, each formulation induces differential levels of cytokines, which creates a unique signature for each of them and thus presents opportunities for using LNPs for vaccination or therapeutic applications.

In the follow-up immunophenotyping analysis, we transfected hPBMCs with all of the mRNA LNP formulations from

https://doi.org/10.1021/acsbiomedchemau.4c00085
ACS Bio Med Chem Au 2025, 5, 154−165

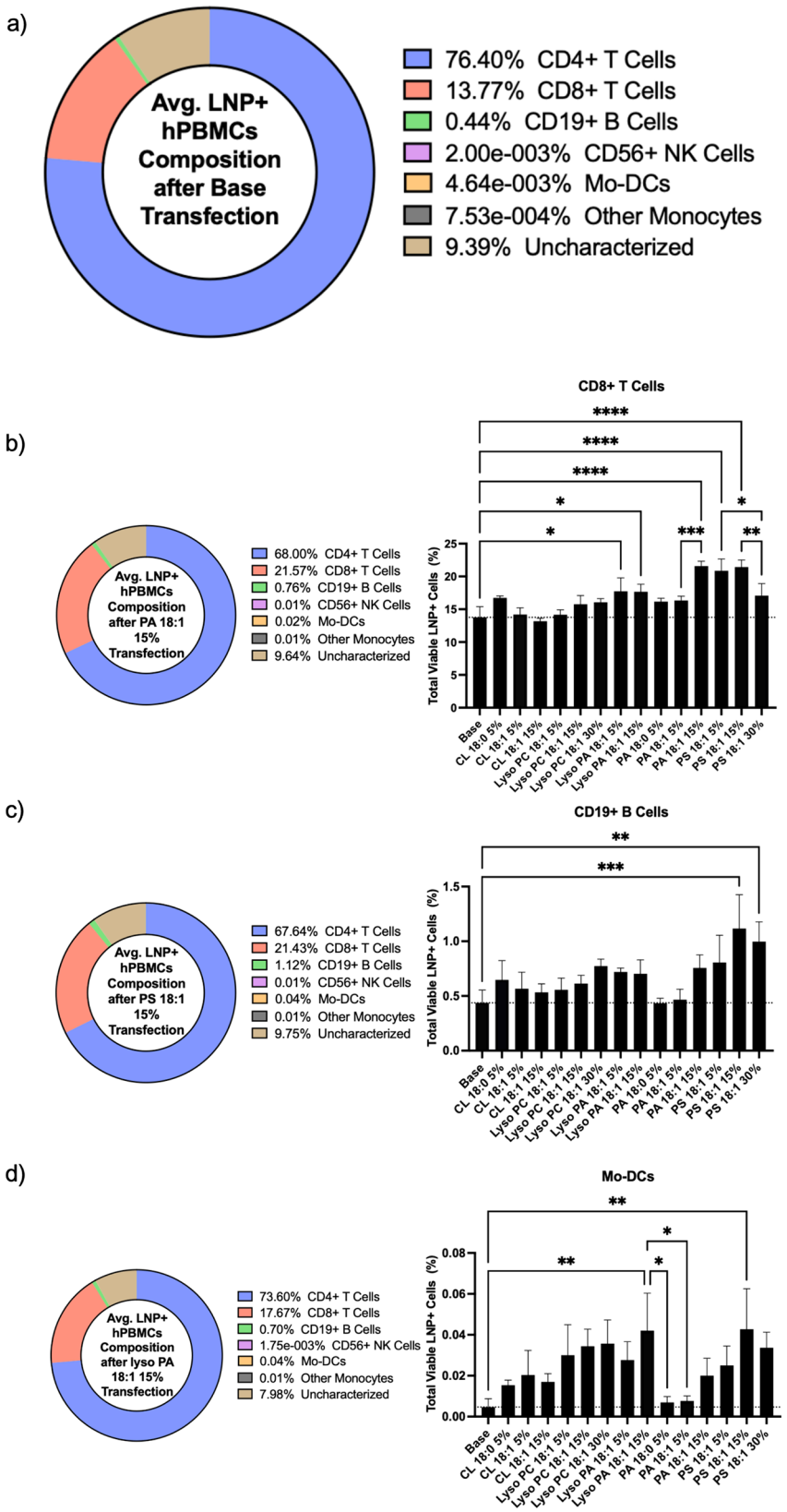

Figure 5. Immunophenotyping of LNP+ hPBMCs of all 14 formulations (0.5 μg of SYTO 13 stained mRNA LNP eGFP). (a) LNP+ hPBMCs composition breakdown after the Base formulation transfection. (b) LNP+ hPBMCs CD8+ T cell proportion change under transfection using different formulations, with 15% PA 18:1 as an example. (c) LNP+ hPBMCs CD19+ B cell proportion change under transfection using different formulations, with 15% PS 18:1 as an example. (d) LNP+ hPBMCs monocyte-derived dendritic cell (Mo-DCs, CD11B+ CD14+ CD11C+ HLA-DR+) proportion change under transfection using different formulations, with 15% lyso PA 18:1 as an example. (b–d) Statistical analysis was conducted using the ordinary one-way ANOVA test followed by Tukey's multiple comparison test. All of the bars represent means ± SD, $n = 3$. Level of significance: $^{*}p \leq 0.05$, $^{**}p \leq 0.01$, $^{***}p \leq 0.001$, $^{****}p \leq 0.0001$.

https://doi.org/10.1021/acsbiomedchemau.4c00085
ACS Bio Med Chem Au 2025, 5, 154–165

the library. Note that these formulations were stained using SYTO 13, a dye that can penetrate LNP membranes and stains for the encapsulated RNA, as the intrinsic eGFP protein expression level within PBMCs was not sufficient for such an analysis (Figure S6b). We validated the hPBMC composition (Figure S6a) and determined the identities of the cells that took up the LNPs using the gating strategies outlined (Figure S5a, b). The composition generally aligned with our expectations of hPBMCs.[46] Note that the culturing and transfection steps may cause population loss for some cell types (Figure S6a), a limitation with our protocol; however, all of the main populations could still be detected with the relative abundance retained (Figure S6a).

Analysis of the LNP+ cells revealed that the majority of the identifiable cells were CD4+ T cells, followed by the CD8+ T cells and the CD19+ B cells, with the CD56+ natural killer (NK) cells being one of the least transfected cell types (Figure 5a). This observation could partly explain the changes associated with those T-cell-affiliated cytokines, such as IL-17 and IL-13, from the previous cytokine response analysis (Figure 4a), further validating the data. Compared to the Base formulation transfection, other formulations demonstrated the potential to slightly change the cellular tropism. For example, both 5% and 15% lyso PA 18:1 formulations enhance LNP uptake in the CD8+ T cells, monocyte-derived dendritic cells (Mo-DCs) and potentially the CD19+ B cells (Figure 5b–d). This aligns with the lyso PA activities associated with both the CD8+ T cells and dendritic cells described in the literature,[47,48] further demonstrating the immunomodulatory potential of the formulations. Similarly, the various PS formulations enhance LNP uptake in the CD8+ T cells, CD19+ B cells, Mo-DCs, other types of monocytes, and potentially even the CD56+ NK cells (Figures 5b–d, S6c). Note that some studies from the literature have reported the mechanistic interactions of PS and NK cells and follow-up technologies to modulate NK cell functions through PS,[49,50] thus further demonstrating the immunomodulatory potential of the PS formulations. Overall, the immunophenotyping study data supplements the cytokine response data to delineate, in greater detail, the potential application areas for the formulations contained in the library.

4. CONCLUSIONS

In conclusion, our study explores the potential of incorporating various levels of different bioactive phospholipids into the current conventional 4-component mRNA LNP formulation and demonstrates the feasibility of such a formulation technique, further expanding the design space of mRNA LNP formulation. These findings further emphasize the critical role of phospholipid in the formulation, not only for structural support of the nanoparticles but also for the biological function-impacting role. Cryo-EM images confirmed the structural similarity between the conventional formulation and the other 5-component formulations. By exploring their potential immunomodulatory effects via cytokine response analysis and immunophenotyping analysis, our work suggests potential novel formulation strategies for RNA therapeutics for altering both the cytokine response and the cellular tropism. As suggested in our previous review,[7] and further enhanced by the data presented here, the lipid components of the LNP formulation could be sensed individually by the cells, which might alter the immune outcomes through direct (e.g., uptake cell identity) and indirect mechanisms (e.g., cytokine release), thus creating an abundant space for immunoengineering design.

ASSOCIATED CONTENT

Supporting Information

The Supporting Information is available free of charge at https://pubs.acs.org/doi/10.1021/acsbiomedchemau.4c00085.

Antibodies used in the immunophenotyping study;18 novel LNP formulations for physicochemical property assessment; quality analysis of mRNA-eGFP samples before LNP formulation using capillary gel electrophoresis analysis; representative cryo-EM images of the formulations in the library; HeLa cell transfection dead cell frequency; cytokine response from human PBMC transfection of all 14 formulations (0.5 μg of mRNA LNP eGFP) using Meso Scale Discovery human U-plex kits; gating strategy for the immunophenotyping experiment; and immunophenotyping of LNP+ hPBMCs (PDF)

AUTHOR INFORMATION

Corresponding Author

Anna K. Blakney − *School of Biomedical Engineering, University of British Columbia, Vancouver V6T 1Z3, Canada; Michael Smith Laboratories, University of British Columbia, Vancouver V6T 1Z4, Canada;* orcid.org/0000-0002-5812-9689; Email: anna.blakney@msl.ubc.ca

Authors

Sunny P. Chen − *School of Biomedical Engineering, University of British Columbia, Vancouver V6T 1Z3, Canada; Michael Smith Laboratories, University of British Columbia, Vancouver V6T 1Z4, Canada;* orcid.org/0000-0002-3278-0449

Shuangyu Wang − *Department of Biochemistry and Molecular Biology, University of British Columbia, Vancouver V6T 2A1, Canada*

Suiyang Liao − *School of Biomedical Engineering, University of British Columbia, Vancouver V6T 1Z3, Canada; Michael Smith Laboratories, University of British Columbia, Vancouver V6T 1Z4, Canada; Department of Biochemistry and Molecular Biology, University of British Columbia, Vancouver V6T 2A1, Canada*

Complete contact information is available at: https://pubs.acs.org/10.1021/acsbiomedchemau.4c00085

Author Contributions

CRediT: **Sunny Peiwei Chen** conceptualization, data curation, formal analysis, investigation, methodology, validation, visualization, writing - original draft, writing - review & editing; **Shuangyu Wang** data curation; **Suiyang Liao** formal analysis, methodology, writing - original draft, writing - review & editing; **Anna K. Blakney** conceptualization, funding acquisition, resources, supervision, visualization, writing - review & editing.

Notes

The authors declare the following competing financial interest(s): The authors, SPC and AKB are both inventors on a provisional patent regarding the use of bioactive phospholipids in LNPs.

https://doi.org/10.1021/acsbiomedchemau.4c00085
ACS Bio Med Chem Au 2025, 5, 154−165

■ ACKNOWLEDGMENTS

We are grateful to Yao Zhang for providing technical insights. This work was supported by Natural Sciences and Engineering Research Council of Canada (NSERC) Discovery Grant, Canadian Institutes of Health Research (CIHR) Operating and Catalyst grants, NanoMedicine Innovative Network (NMIN) Grand Challenge grant, NMIN Graduate Award to SPC, MSFHR Scholar Award to AKB and Tier II Canada Research Chair to AKB.

■ REFERENCES

(1) U.S. Food and Drug Administration. ONPATTRO FULL PRESCRIBING INFORMATION. 2018. URL: https://www.accessdata.fda.gov/drugsatfda_docs/label/2018/210922s000lbl.pdf (acccessed 8/29/2024).
(2) U.S. Food and Drug Administration. Moderna COVID-19 Vaccine EUA Letter of Authorization. 2024. URL: https://www.fda.gov/media/144636/download?attachment (acccessed 8/29/2024).
(3) U.S. Food and Drug Administration. Pfizer-BioNTech COVID-19 Vaccine EUA LOA reissued. 2024. URL: https://www.fda.gov/media/150386/download?attachment (acccessed 8/29/2024).
(4) Mullard, A. FDA approves mRNA-based RSV vaccine. *Nature reviews drug discovery* **2024**, *23*, 487−488.
(5) Hou, X.; Zaks, T.; Langer, R.; Dong, Y. Lipid nanoparticles for mRNA delivery. *Nat. Rev. Mater.* **2021**, *6* (12), 1078−1094.
(6) Aldosari, B. N.; Alfagih, I. M.; Almurshedi, A. S. Lipid Nanoparticles as Delivery Systems for RNA-Based Vaccines. *Pharmaceutics* **2021**, *13* (2), 206.
(7) Chen, S. P.; Blakney, A. K. Immune response to the components of lipid nanoparticles for ribonucleic acid therapeutics. *Curr. Opin Biotechnol* **2024**, *85*, 103049.
(8) Tam, A.; Kulkarni, J.; An, K.; Li, L.; Dorscheid, D. R.; Singhera, G. K.; Bernatchez, P.; Reid, G.; Chan, K.; Witzigmann, D.; et al. Lipid nanoparticle formulations for optimal RNA-based topical delivery to murine airways. *Eur. J. Pharm. Sci.* **2022**, *176*, 106234.
(9) Luozhong, S.; Yuan, Z.; Sarmiento, T.; Chen, Y.; Gu, W.; McCurdy, C.; Gao, W.; Li, R.; Wilkens, S.; Jiang, S. Phosphatidylserine Lipid Nanoparticles Promote Systemic RNA Delivery to Secondary Lymphoid Organs. *Nano Lett.* **2022**, *22* (20), 8304−8311.
(10) Cheng, Q.; Wei, T.; Farbiak, L.; Johnson, L. T.; Dilliard, S. A.; Siegwart, D. J. Selective organ targeting (SORT) nanoparticles for tissue-specific mRNA delivery and CRISPR-Cas gene editing. *Nat. Nanotechnol* **2020**, *15* (4), 313−320.
(11) Alvarez-Benedicto, E.; Farbiak, L.; Marquez Ramirez, M.; Wang, X.; Johnson, L. T.; Mian, O.; Guerrero, E. D.; Siegwart, D. J. Optimization of phospholipid chemistry for improved lipid nanoparticle (LNP) delivery of messenger RNA (mRNA). *Biomater Sci.* **2022**, *10* (2), 549−559.
(12) Liu, S.; Cheng, Q.; Wei, T.; Yu, X.; Johnson, L. T.; Farbiak, L.; Siegwart, D. J. Membrane-destabilizing ionizable phospholipids for organ-selective mRNA delivery and CRISPR-Cas gene editing. *Nat. Mater.* **2021**, *20* (5), 701−710.
(13) Zhou, F.; Huang, L.; Li, S.; Yang, W.; Chen, F.; Cai, Z.; Liu, X.; Xu, W.; Lehto, V.-P.; Lächelt, U.; et al. From structural design to delivery: mRNA therapeutics for cancer immunotherapy. *Exploration* **2024**, *4* (2), 20210146.
(14) O'Donnell, V. B.; Rossjohn, J.; Wakelam, M. J. Phospholipid signaling in innate immune cells. *J. Clin Invest* **2018**, *128* (7), 2670−2679.
(15) Miao, L.; Li, L.; Huang, Y.; Delcassian, D.; Chahal, J.; Han, J.; Shi, Y.; Sadtler, K.; Gao, W.; Lin, J.; et al. Delivery of mRNA vaccines with heterocyclic lipids increases anti-tumor efficacy by STING-mediated immune cell activation. *Nat. Biotechnol.* **2019**, *37* (10), 1174−1185.
(16) Nguyen, N. H.; Glassman, F. Y.; Dingman, R. K.; Shenoy, G. N.; Wohlfert, E. A.; Kay, J. G.; Bankert, R. B.; Balu-Iyer, S. V. Rational design of a nanoparticle platform for oral prophylactic immunotherapy to prevent immunogenicity of therapeutic proteins. *Sci. Rep* **2021**, *11* (1), 17853.
(17) Pizzuto, M.; Lonez, C.; Baroja-Mazo, A.; Martinez-Banaclocha, H.; Tourlomousis, P.; Gangloff, M.; Pelegrin, P.; Ruysschaert, J. M.; Gay, N. J.; Bryant, C. E. Saturation of acyl chains converts cardiolipin from an antagonist to an activator of Toll-like receptor-4. *Cell. Mol. Life Sci.* **2019**, *76* (18), 3667−3678.
(18) Knuplez, E.; Marsche, G. An Updated Review of Pro- and Anti-Inflammatory Properties of Plasma Lysophosphatidylcholines in the Vascular System. *International Journal of Molecular Sciences* **2020**, *21* (12), 4501.
(19) Fan, H.; Zingarelli, B.; Harris, V.; Tempel, G. E.; Halushka, P. V.; Cook, J. A. Lysophosphatidic acid inhibits bacterial endotoxin-induced pro-inflammatory response: potential anti-inflammatory signaling pathways. *Mol. Med.* **2008**, *14* (7−8), 422−428.
(20) Lee, Y. N.; Lee, H. Y.; Kang, H. K.; Kwak, J. Y.; Bae, Y. S. Phosphatidic acid positively regulates LPS-induced differentiation of RAW264.7 murine macrophage cell line into dendritic-like cells. *Biochem. Biophys. Res. Commun.* **2004**, *318* (4), 839−845.
(21) Ly, H. H.; Daniel, S.; Soriano, S. K. V.; Kis, Z.; Blakney, A. K. Optimization of Lipid Nanoparticles for saRNA Expression and Cellular Activation Using a Design-of-Experiment Approach. *Mol. Pharmaceutics* **2022**, *19* (6), 1892−1905.
(22) Kauffman, K. J.; Dorkin, J. R.; Yang, J. H.; Heartlein, M. W.; DeRosa, F.; Mir, F. F.; Fenton, O. S.; Anderson, D. G. Optimization of Lipid Nanoparticle Formulations for mRNA Delivery in Vivo with Fractional Factorial and Definitive Screening Designs. *Nano Lett.* **2015**, *15* (11), 7300.
(23) Hald Albertsen, C.; Kulkarni, J. A.; Witzigmann, D.; Lind, M.; Petersson, K.; Simonsen, J. B. The role of lipid components in lipid nanoparticles for vaccines and gene therapy. *Adv. Drug Deliv Rev.* **2022**, *188*, 114416.
(24) Simonsen, J. B. A perspective on bleb and empty LNP structures. *J. Controlled Release* **2024**, *373*, 952−961.
(25) Cheng, M. H. Y.; Leung, J.; Zhang, Y.; Strong, C.; Basha, G.; Momeni, A.; Chen, Y.; Jan, E.; Abdolahzadeh, A.; Wang, X.; et al. Induction of Bleb Structures in Lipid Nanoparticle Formulations of mRNA Leads to Improved Transfection Potency. *Adv. Mater.* **2023**, *35* (31), No. e2303370.
(26) Masuda, M.; Miyazaki-Anzai, S.; Keenan, A. L.; Okamura, K.; Kendrick, J.; Chonchol, M.; Offermanns, S.; Ntambi, J. M.; Kuro, O. M.; Miyazaki, M. Saturated phosphatidic acids mediate saturated fatty acid-induced vascular calcification and lipotoxicity. *J. Clin Invest* **2015**, *125* (12), 4544−4558.
(27) Qi, C.; Park, J.-H.; Gibbs, T. C.; Shirley, D. W.; Bradshaw, C. D.; Ella, K. M.; Meier, K. E. Lysophosphatidic acid stimulates phospholipase D activity and cell proliferation in PC-3 human prostate cancer cells. *Journal of Cellular Physiology* **1998**, *174* (2), 261−272.
(28) Xu, Y.; Fang, X. J.; Casey, G.; Mills, G. B. Lysophospholipids activate ovarian and breast cancer cells. *Biochem. J.* **1995**, *309* (3), 933−940.
(29) Lotter, C.; Alter, C. L.; Bolten, J. S.; Detampel, P.; Palivan, C. G.; Einfalt, T.; Huwyler, J. Incorporation of phosphatidylserine improves efficiency of lipid based gene delivery systems. *Eur. J. Pharm. Biopharm* **2022**, *172*, 134−143.
(30) Bakos, T.; Mészáros, T.; Kozma, G. T.; Berényi, P.; Facskó, R.; Farkas, H.; Dézsi, L.; Heirman, C.; de Koker, S.; Schiffelers, R.; et al. mRNA-LNP COVID-19 Vaccine Lipids Induce Complement Activation and Production of Proinflammatory Cytokines: Mechanisms, Effects of Complement Inhibitors, and Relevance to Adverse Reactions. *International Journal of Molecular Sciences* **2024**, *25* (7), 3595.
(31) Dobrovolskaia, M. A.; Afonin, K. A. Use of human peripheral blood mononuclear cells to define immunological properties of nucleic acid nanoparticles. *Nat. Protoc* **2020**, *15* (11), 3678−3698.
(32) Lim, H. K.; Choi, Y. A.; Park, W.; Lee, T.; Ryu, S. H.; Kim, S. Y.; Kim, J. R.; Kim, J. H.; Baek, S. H. Phosphatidic acid regulates systemic inflammatory responses by modulating the Akt-mammalian

https://doi.org/10.1021/acsbiomedchemau.4c00085
ACS Bio Med Chem Au 2025, 5, 154−165

target of rapamycin-p70 S6 kinase 1 pathway. *J. Biol. Chem.* **2003**, *278* (46), 45117−45127.
(33) Reynolds, M. B.; Hong, H. S.; Michmerhuizen, B. C.; Lawrence, A. E.; Zhang, L.; Knight, J. S.; Lyssiotis, C. A.; Abuaita, B. H.; O'Riordan, M. X. Cardiolipin coordinates inflammatory metabolic reprogramming through regulation of Complex II disassembly and degradation. *Sci. Adv.* **2023**, *9* (5), No. eade8701.
(34) Xu, X.; Wang, X.; Liao, Y. P.; Luo, L.; Xia, T.; Nel, A. E. Use of a Liver-Targeting Immune-Tolerogenic mRNA Lipid Nanoparticle Platform to Treat Peanut-Induced Anaphylaxis by Single- and Multiple-Epitope Nucleotide Sequence Delivery. *ACS Nano* **2023**, *17* (5), 4942−4957.
(35) Gaitonde, P.; Peng, A.; Straubinger, R. M.; Bankert, R. B.; Balu-Iyer, S. V. Phosphatidylserine reduces immune response against human recombinant Factor VIII in Hemophilia A mice by regulation of dendritic cell function. *Clin Immunol* **2011**, *138* (2), 135−145.
(36) Liu, H.; Chen, Y. G. The Interplay Between TGF-β Signaling and Cell Metabolism. *Front Cell Dev Biol.* **2022**, *10*, 846723.
(37) Sanjabi, S.; Zenewicz, L. A.; Kamanaka, M.; Flavell, R. A. Anti-inflammatory and pro-inflammatory roles of TGF-beta, IL-10, and IL-22 in immunity and autoimmunity. *Curr. Opin Pharmacol* **2009**, *9* (4), 447−453.
(38) Tanaka, T.; Narazaki, M.; Kishimoto, T. IL-6 in inflammation, immunity, and disease. *Cold Spring Harb Perspect Biol.* **2014**, *6* (10), a016295.
(39) Alameh, M. G.; Tombacz, I.; Bettini, E.; Lederer, K.; Sittplangkoon, C.; Wilmore, J. R.; Gaudette, B. T.; Soliman, O. Y.; Pine, M.; Hicks, P.; et al. Lipid nanoparticles enhance the efficacy of mRNA and protein subunit vaccines by inducing robust T follicular helper cell and humoral responses. *Immunity* **2021**, *54* (12), 2877−2892.
(40) York, A. G.; Skadow, M. H.; Oh, J.; Qu, R.; Zhou, Q. D.; Hsieh, W.-Y.; Mowel, W. K.; Brewer, J. R.; Kaffe, E.; Williams, K. J.; et al. IL-10 constrains sphingolipid metabolism to limit inflammation. *Nature* **2024**, *627* (8004), 628−635.
(41) Pizzuto, M.; Pelegrin, P. Cardiolipin in Immune Signaling and Cell Death. *Trends Cell Biol.* **2020**, *30* (11), 892−903.
(42) Khorrami, A.; Ziaee, M.; Rameshrad, M.; Nakhlband, A.; Maleki-Dizaji, N.; Garjani, A. Oxidized cholesterol exacerbates toll-like receptor 4 expression and activity in the hearts of rats with myocardial infarction. *J. Cardiovasc Thorac Res.* **2020**, *12* (1), 43−50.
(43) Zhao, Y.; He, D.; Zhao, J.; Wang, L.; Leff, A. R.; Spannhake, E. W.; Georas, S.; Natarajan, V. Lysophosphatidic acid induces interleukin-13 (IL-13) receptor alpha2 expression and inhibits IL-13 signaling in primary human bronchial epithelial cells. *J. Biol. Chem.* **2007**, *282* (14), 10172−10179.
(44) Park, G. Y.; Lee, Y. G.; Berdyshev, E.; Nyenhuis, S.; Du, J.; Fu, P.; Gorshkova, I. A.; Li, Y.; Chung, S.; Karpurapu, M.; et al. Autotaxin production of lysophosphatidic acid mediates allergic asthmatic inflammation. *Am. J. Respir Crit Care Med.* **2013**, *188* (8), 928−940.
(45) Rubenfeld, J.; Guo, J.; Sookrung, N.; Chen, R.; Chaicumpa, W.; Casolaro, V.; Zhao, Y.; Natarajan, V.; Georas, S. Lysophosphatidic acid enhances interleukin-13 gene expression and promoter activity in T cells. *American Journal of Physiology-Lung Cellular and Molecular Physiology* **2006**, *290* (1), L66−L74.
(46) Autissier, P.; Soulas, C.; Burdo, T. H.; Williams, K. C. Evaluation of a 12-color flow cytometry panel to study lymphocyte, monocyte, and dendritic cell subsets in humans. *Cytometry A* **2010**, *77* (5), 410−419.
(47) Turner, J. A.; Fredrickson, M. A.; D'Antonio, M.; Katsnelson, E.; MacBeth, M.; Van Gulick, R.; Chimed, T. S.; McCarter, M.; D'Alessandro, A.; Robinson, W. A.; et al. Lysophosphatidic acid modulates CD8 T cell immunosurveillance and metabolism to impair anti-tumor immunity. *Nat. Commun.* **2023**, *14* (1), 3214.
(48) Panther, E.; Idzko, M.; Corinti, S.; Ferrari, D.; Herouy, Y.; Mockenhaupt, M.; Dichmann, S.; Gebicke-Haerter, P.; Di Virgilio, F.; Girolomoni, G.; et al. The influence of lysophosphatidic acid on the functions of human dendritic cells. *J. Immunol* **2002**, *169* (8), 4129−4135.
(49) Tan, S.; Xu, Y.; Wang, Z.; Wang, T.; Du, X.; Song, X.; Guo, X.; Peng, J.; Zhang, J.; Liang, Y.; et al. Tim-3 Hampers Tumor Surveillance of Liver-Resident and Conventional NK Cells by Disrupting PI3K Signaling. *Cancer Res.* **2020**, *80* (5), 1130−1142.
(50) Yang, X.; Li, M.; Qin, X.; Tan, S.; Du, L.; Ma, C.; Li, M. Photophosphatidylserine Guides Natural Killer Cell Photoimmunotherapy via Tim-3. *J. Am. Chem. Soc.* **2022**, *144* (9), 3863−3874.

https://doi.org/10.1021/acsbiomedchemau.4c00085
ACS Bio Med Chem Au 2025, 5, 154−165